

FNBP4 is a Potential Biomarker Associated with Cuproptosis and Promotes Tumor Progression in Hepatocellular Carcinoma

Kai-Wen Zheng^{1,2}, Chao-Hua Zhang³, Wu Wu¹, Zhu Zhu¹, Jian-Ping Gong¹, Chun-Ming Li¹

¹Department of Hepatobiliary Surgery, the Second Affiliated Hospital of Chongqing Medical University, Chongqing, People's Republic of China;

²Department of Hepatobiliary Surgery, the People's Hospital of Rongchang District, Chongqing, People's Republic of China; ³Department of Gastrointestinal Surgery, the Second Affiliated Hospital of Chongqing Medical University, Chongqing, People's Republic of China

Correspondence: Chun-Ming Li, Email lcm2021518@163.com

Background: Hepatocellular carcinoma (HCC) is one of the most common malignant tumors that lacks an efficient therapeutic approach because of its elusive molecular mechanisms. This study aimed to investigate the biological function and potential mechanism of formin-binding protein 4 (FNBP4) in HCC.

Methods: FNBP4 expression in tissues and cells were detected by quantitative real-time PCR (qRT-PCR), Western blot, and immunohistochemistry (IHC). The Kaplan-Meier method was used to explore the correlation between the FNBP4 expression and clinical survival. MTT, EdU incorporation, colony formation, and Transwell assays were performed to evaluate the function of FNBP4 in cell proliferation and migration in vitro. Kyoto Encyclopedia of Genes and Genomes (KEGG) pathway analysis was used to explore the potential mechanism of FNBP4. The prognostic risk signature and nomogram were constructed to demonstrate the prognostic value of FNBP4.

Results: We found that FNBP4 was upregulated in patients with HCC and associated with poor overall survival (OS). Furthermore, knockdown of FNBP4 inhibited the proliferation and migration in HCC cells. Then, we performed a KEGG pathway analysis of the coexpressed genes associated with FNBP4 and found that FNBP4 may be associated with tumor-related signaling pathways and cuproptosis. We verified that FNBP4 could cause cell cycle progression and inactivation of the hippo signaling pathway. A prognostic risk signature containing three FNBP4-related differentially expressed cuproptosis regulators (DECs) was established and can be used as an independent risk factor to evaluate the prognosis of patients with HCC. In addition, a nomogram including a risk score and clinicopathological factors was used to predict patient survival probabilities.

Conclusion: FNBP4, as a potential biomarker associated with cuproptosis, promotes HCC cell proliferation and metastasis. We provide a new potential strategy for HCC treatment by targeting FNBP4.

Keywords: FNBP4, hepatocellular carcinoma, HCC, cuproptosis, biomarker

Introduction

Liver cancer ranks sixth among all cancers and is the third leading cause of cancer-related death worldwide.¹ Hepatocellular carcinoma (HCC) accounts for 90% of primary liver cancers and causes approximately 800,000 deaths annually,^{2,3} which is a serious burden to human health. Hepatitis viral infection, alcohol accumulation, and non-alcoholic fatty liver disease (NAFLD) are the main risk factors for HCC. However, its etiology and molecular mechanism are still unclear. In addition, once patients have symptoms and signs, the disease has progressed to the late stages, and patients have lost the opportunity for radical surgical treatment. Systemic therapies have been used in approximately 50% of patients with HCC and become standard treatment options for patients with advanced HCC.⁴ In recent years, immunotherapy and molecular targeted therapy have also been developed and are expected to become new treatment methods. Immune checkpoint inhibitors (ICIs) (pembrolizumab, nivolumab, durvalumab, atezolizumab, etc.) have been recently evaluated in HCC patients and clinical trials assessing single-agent ICI have reported disappointing results. Conversely, immune-based combinations have received statistically significant and clinically meaningful benefits in several clinical

outcomes.^{5,6} In particular, a recent clinical trial showed a longer median OS in HCC patients across all age groups receiving the PD-L1 inhibitor atezolizumab plus the antiangiogenic agent bevacizumab.⁷ However, the population reached by immunotherapy is far from satisfactory. Although studies provided some potentially useful predictive biomarkers of response to immunotherapy in HCC,^{8,9} further validations and interpretations are needed. In addition, clinical trials on molecular targeted drugs (sorafenib, lenvatinib, regorafenib, cabozantinib, etc.) have been widely conducted, but several adverse events still constrain their clinical application.^{10,11} Therefore, it is urgent to identify new targets for the treatment of liver cancer.

Formins promote the initiation and elongation of actin filaments to participate in a variety of biological processes, such as cell signaling, organ development, microtubule stabilization, cell division, and endocytosis.^{12–15} Formin-mediated actin assembly is regulated by a protein family consisting of formin-binding proteins (FNBPs/FBPs). Previous studies showed that the high expression of FBNP1 is closely related to the highly aggressive characteristics of tumor cells within gastric and breast cancers.^{16,17} FBNP4, also named FBP30, is located on 11p14 and is a member of the FBP family. This gene encodes a protein containing two tryptophan-rich WW domains that bind the proline-rich formin homology 1 domains of formin family proteins, suggesting a role in the regulation of cytoskeletal dynamics during cell division and migration. A study found that FBNP4 as a p53 regulated protein, which is highly expressed in apoptotic mouse T cells, and the authors speculated about the possible role of this protein in cell death.¹⁸ However, the expression level and function of FBNP4 in various tumors including HCC remain unknown.

Copper is an important nutrient involved in a variety of biological functions including mitochondrial respiration, oxidative stress, and cytotoxicity.^{19–21} Dysregulation of copper homeostasis has been associated with tumor proliferation, angiogenesis, and metastasis, suggesting that copper may play a role in tumor progression.^{22–24} Studies have found that liver copper content is closely related to HCC, and serum copper and ceruloplasmin levels could be used as markers for HCC detection.²⁵ Recently, cuproptosis, a novel copper-triggered mode of mitochondrial cell death, is closely associated with protein lipoylation in the tricarboxylic acid (TCA) cycle, providing insights into new therapies for HCC.²⁶ Researchers also identified ferredoxin 1 (FDX1) as an upstream regulator of protein lipoylation to mediate copper toxicity. Several studies have found that copper death-related genes are closely related to the tumor microenvironment and prognosis of HCC.^{27–29} Furthermore, studies have suggested that copper ionophores could be anticancer agents.^{30,31} However, lack of selectivity is one of the major barriers in the field; thus, future research should be devoted to exploring specific targets for copper metabolism in tumor cells.

In this study, we found that FBNP4 was upregulated in patients with HCC and HCC cell lines. High expression of FBNP4 was also related to the poor OS of patients with HCC. In addition, downregulation of FBNP4 inhibited the proliferation and migration of HCC cells. Furthermore, we constructed a prognostic risk signature based on FBNP4-related cuproptosis regulators. The risk signature, as an independent risk factor for OS, had good evaluation efficacy for determining the clinical prognosis of patients with HCC. Therefore, our study provides a significant biomarker for the treatment and prognostic evaluation of HCC.

Materials and Methods

Data Collection

Transcriptome data (n = 424) and clinical and pathological characteristics (n = 377) including tumor grade, age, sex, Tumor, Node, Metastasis (TNM) stage, survival time, and survival condition were collected from The Cancer Genome Atlas-Liver hepatocellular carcinoma (TCGA-LIHC) database (<https://portal.gdc.cancer.gov/>). Fragments per kilobase million (FPKM) were used for the transcriptome data. After excluding patients with missing survival data and crucial clinical data, 370 samples were retained for further analysis. Transcriptome data were used to analyze the expression levels of FBNP4. The 10 cuproptosis regulators identified by Tsvetkov et al²⁶ were used in our study. As an open-source database, each case involved in TCGA has gained ethical agreement and has been approved by TCGA.

Expression and Survival Analysis of FBNP4

The Gene Expression Profiling Interactive Analysis 2 (GEPIA2) (<http://gepia2.cancer-pku.cn/>) was used to analyze the expression levels and prognostic value of FBNP4 in patients with HCC.

Coexpressed Gene Prediction and Gene Set Enrichment Analysis (GSEA)

LinkedOmics (<http://www.linkedomics.org/>) includes multi-omics data for 32 cancers derived from TCGA. The coexpressed genes of FNBP4 and their correlations were analyzed using LinkFinder's LinkedOmics. A KEGG pathway analysis of FNBP4 coexpressed genes was performed using GSEA tools in LinkInterpreter's LinkedOmics.

Construction of the Prognostic Signature and Nomogram

Analysis of differential mRNA expression of cuproptosis regulators was performed by R package “limma” in FNBP4 low and FNBP4 high HCC samples from TCGA-LIHC database. A prognostic signature was established based on FNBP4-related differentially expressed cuproptosis regulators (DECRs) using Cox regression analysis. Risk scores were calculated using the following formula: $\text{risk score} = \beta_1x_1 + \beta_2x_2 + \dots + \beta_nx_n$, where β_i denotes the gene coefficient, and x_i denotes the gene expression level. A Kaplan-Meier survival curve was used to assess the association between risk score and OS of patients with HCC. Univariate and multivariate Cox regression analyses were performed to determine whether the risk score is an independent prognosis risk factor of the OS. The predictive performance of the risk score was evaluated using receiver operating characteristic (ROC) curves. A nomogram including the risk score and clinicopathological characteristics was constructed to predict the OS of patients with HCC using the R package “rms”. Calibration curves were constructed to compare the predicated OS with the actual OS using the R package “rms”.

Patients and Tissue Samples

Tissue samples were collected from 10 patients with HCC at the Department of Hepatobiliary Surgery at the Second Affiliated Hospital of Chongqing Medical University for subsequent mRNA and protein detection. Written informed consent for the collection of tissue samples was obtained from the patients. The study was approved by the Ethics Committee of the Second Affiliated Hospital of Chongqing Medical University and complied with the Declaration of Helsinki.

Cell Culture and Transfection

The five HCC cell lines (LM3, HepG2, Hep3B, SMMC-7721, and Huh7) and the hepatocyte cell line LO2 were purchased from the Institute of Biochemistry and Cell Biology (Shanghai, China). All cell lines were cultured with Dulbecco's modified Eagle's medium (Gibco, USA) containing 10% fetal bovine serum (Gibco, USA) and 100 units/mL penicillin and streptomycin (HyClone, USA) in a humidified incubator at 37°C with 5% CO₂. Lipofectamine 2000 (Invitrogen, 11668019) was used for FNBP4 small interfering RNA (siRNA) or negative control siRNA transfection based on the manufacturer's instructions. Briefly, transfection began when the cells were 70–90% confluent. For a well in a six-well plate, 4 µL Lipofectamine 2000 and siRNA (100 pmol) were respectively diluted in 100 µL Opti-MEM (Gibco, USA), and diluted siRNA was added to diluted Lipofectamine 2000. After incubation for 15 mins, the siRNA-Lipo complex was added to cells and the cells were incubated for 1–3 days for the subsequent experiment. FNBP4 siRNA-1 (5'-AGGGATCATAGACGGTATTTC-3'), FNBP4 siRNA-2 (5'-CCACAGTTGTAAGTAGCCAGA-3'), and its associated control siRNA were obtained from GenePharma (Shanghai, China).

Quantitative Real-Time PCR (qRT-PCR)

Trizol Reagent (Invitrogen, 15596018) was used to extract the total RNA from HCC tissues and HCC cell lines. Then, the RNA was reverse transcribed into cDNA using the PrimeScript RT Reagent kit (TaKaRa) according to the manufacturer's instructions. Tissues and cell mRNA expression levels were measured by qRT-PCR using TB Green Premix Ex Taq II (TaKaRa). The PCR cycle programs were as follows: 95°C for 30s, followed by 40 cycles at 95°C for 5 s and 60°C for 1 min. β -actin was used as the internal control. The experimental sequence primers used are as follows: 5'-TTGGTGCTTATGCTGACAGTG-3' (forward) and 5'-GATCTCCGCTAGGAAGTTGGC-3' (reverse) for FNBP4 and 5'-CCTTCCTGGGCATGGAGTCCT-3' (forward) and 5'-GGAGCAATGATCTTGATCTT-3' (reverse) for β -actin.

Western Blot Assay

The total proteins of HCC tissues or cells were extracted using RIPA lysis buffer (Beyotime, China) and the protein concentration was determined using a bicinchoninic acid kit (Beyotime, China) according to the manufacturer's instructions. The proteins were separated by polyacrylamide gel electrophoresis and transferred to a nitrocellulose transfer membrane (GE Healthcare, USA). The membranes were incubated overnight at 4°C with the following specific primary antibodies: FBNP4 (Invitrogen, PA5-59035, 1:1000), β -actin (Proteintech, 60008-1-Ig, 1:5000), LAST1 (Abcam, ab70561, 1:5000), p-YAP (Abcam, ab76252, 1:5000), YAP (Abcam, ab52771, 1:5000), p53 (CST, 2524, 1:1000), p21 (CST, 2947, 1:1000), Cyclin B1 (CST, 12231, 1:1000), Cyclin D1 (CST, 2978, 1:1000), and Cyclin A2 (CST, 67955, 1:1000). After washing three times with TBST, the membranes were incubated with anti-rabbit immunoglobulin G (IgG) (CST, 7074, 1:5000) or anti-mouse immunoglobulin G (IgG) (CST, 7076, 1:5000) secondary antibody at room temperature for 1 hr. After washing again, the protein bands were visualized using an Image Analysis System (Bio-Rad, USA) with an Enhanced Chemiluminescence Fluorescence Detection kit (GE HealthCare, USA).

Immunohistochemistry

Paraffin-embedded tissues from HCC patients were cut into three μ m slices. Antigen repair was performed by high temperature and high pressure with sodium citrate solution (Beyotime, China). Endogenous peroxidase was inactivated with 3% hydrogen peroxide solution for 10 mins and then blocked with goat serum at room temperature for 30 mins. Then, the sections were incubated overnight at 4°C with the FBNP4 (Invitrogen, PA5-59035, 1:200) specific primary antibody. After incubating goat anti-rabbit secondary antibody at room temperature for 30 mins, immunohistochemistry (IHC) was performed using a polymer horseradish peroxidase detection system (Zhongshan Goldenbridge Biotechnology, China) and the sections were photographed by an inverted microscope (Olympus, BX41).

MTT, 5-Ethynyl-2'-Deoxyuridine (EdU) Incorporation, and Colony-Forming Assays

The MTT, EdU incorporation, and colony-forming assays were used to analyze cell proliferation. Huh7 and Hep3B cells were seeded in 96-well plates at 3000 cells per well. A total of 10 μ L of MTT reagent (5mg/mL, Solarbio, China) was added to each well at 0, 24, 48, and 72 hrs after transfection, and the cells were then incubated at 37°C for 3 hrs. Then, the culture medium was removed from the wells, and 100 μ L of DMSO was added to each well to dissolve the formazan. The absorbance at 490 nm was detected using an enzyme calibration system (ThermoFisher Scientific, USA). The EdU incorporation assay was performed according to the manufacturer's instructions for the BeyoClick™ EdU Cell Proliferation Kit with Alexa Fluor 488 (Beyotime, China). Huh7 and Hep3B (5×10^4 cells/well) cells were transfected in 24-well plates for 24 hrs. After incubation with EdU (10 μ M) at 37°C for 2 hrs, the cells were treated with 4% formaldehyde for 15 mins, and 3% bovine serum albumin (BSA) was used to remove the fixed solution. Then, the cells were permeated with 0.3% Triton X-100 solution for 10 mins and washed twice with 3% BSA. The click additive solution was added for 30 mins, and $1 \times$ Hoechst 33342 was used to stain the nuclei for 10 mins in the dark. The number of EdU-positive cells was measured using ImageJ. Huh7 and Hep3B cells (1000 cells/well) were seeded in 6-well plates and cultured for two weeks to form a colony composed of at least 50 cells. The colonies were fixed in 4% formaldehyde for 15 mins and stained with 0.1% crystal violet for 30 mins. The number of colonies was counted using microscopy.

Transwell Assay

To perform the Transwell assay, 24-well Transwell chambers (Corning, USA) were used to assess cell migration. Huh7 and Hep3B cells (1000 cells/well) were seeded in the upper chamber at 1×10^5 cells per group with 200 μ L of serum-free medium. The lower chamber was filled with 500 μ L of complete medium with 10% FBS. After 24 hrs, the Transwell chambers were fixed in 4% formaldehyde for 15 mins and stained with 0.1% crystal violet for 30 mins. The migrated cells were photographed with inverted microscopy and measured with ImageJ.

Statistical Analysis

GraphPad Prism 8 and R (v4.0.5) were used to analyze the trial data. The Kaplan-Meier method was performed for survival analysis. Spearman's method was used to analyze the coexpressed genes of FNBP4. Univariate and multivariate Cox regression models were used to determine the independent prognostic factors. The *t*-test was used to compare the differences between the two groups, and ANOVA was used when more than two groups were compared. All measurement data are expressed as the mean \pm SEM. A P-value < 0.05 indicated statistical significance.

Results

FNBP4 is Highly Expressed in Patients with HCC and is Positively Correlated with Poor OS

The current study used the TCGA database to analyze the mRNA expression, and the results demonstrated that FNBP4 was upregulated in HCC samples compared with normal samples (Figure 1A). The expression of FNBP4 was positively correlated with the pathological stage (Figure 1B). In addition, both mRNA and protein levels of FNBP4 were increased in 10 HCC tissues compared with paired adjacent tissues from our center (Figure 1C-E). We also found that the expression levels of FNBP4 in five HCC cell lines were increased compared with those in the normal hepatocyte cell line LO2 (Figure 1F). Kaplan-Meier analysis showed that high expression levels of FNBP4 were associated with poor OS in patients with HCC, indicating that FNBP4 exerted a significant effect on the survival of patients with HCC (Figure 1G). These results indicated that FNBP4 is highly expressed in HCC and is positively correlated with the poor OS of patients with HCC.

Knockdown of FNBP4 Inhibits the Proliferation and Migration of HCC Cells

To explore the function of FNBP4 on HCC proliferation and metastasis, Huh7 and Hep3B cells with high expression levels of FNBP4 were used for further study. First, siFNBP4 was used to knockdown FNBP4 expression in HCC cells, and qRT-PCR was used to test the knockdown efficiency (Figure 2A). The results revealed that knockdown of FNBP4 significantly reduced FNBP4 expression. Furthermore, knockdown of FNBP4 significantly inhibited cell proliferation, as indicated by the MTT, EdU incorporation, and colony formation assays (Figure 2B-F). In addition, we found that silencing of FNBP4 significantly inhibited cell migration in Huh7 and Hep3B cells using a Transwell assay (Figure 2G-H). Thus, knockdown of FNBP4 inhibits HCC cell proliferation and migration.

FNBP4 is Associated with Tumor-Related Signaling Pathways and Cuproptosis Regulators in HCC

To further explore the potential mechanism of action of FNBP4 in HCC, coexpressed genes of FNBP4 were analyzed by a KEGG pathway analysis. First, we identified FNBP4 coexpressed genes using RNA-seq data in TCGA-LIHC. The heat map presents the 50 positively and negatively correlated genes with the highest associations with FNBP4 (Supplementary Figure 1). Then, a KEGG pathway analysis of FNBP4 coexpressed genes was performed using LinkedOmics (Figure 3A). FNBP4 coexpressed genes were mainly enriched in tumor-related signaling pathways including microRNA in cancer, the GnRH signaling pathway, the cell cycle, and the hippo signaling pathway. The protein expression levels of cell cycle-associated markers (p53, p21, Cyclin B1, Cyclin D1, and Cyclin A2) and the hippo signaling pathway components (LAST1, p-YAP, and YAP) were measured in Huh7 and Hep3B cells transfected with siCtrl or siFNBP4. We found that silencing of FNBP4 downregulated levels of YAP and Cyclin D1, and upregulated the levels of p53, p21, LAST1, and p-YAP, indicating that FNBP4 causes cell cycle progression and inactivation of the hippo signaling pathway (Figure 3B). Interestingly, FNBP4 coexpressed genes were involved in TCA cycle-related pathways including carbon metabolism, metabolism of xenobiotics by cytochrome P450, and oxidative phosphorylation. As the TCA cycle is closely related to cuproptosis,³² FNBP4 may influence HCC progression through cuproptosis. Therefore, we explored the relationship between FNBP4 and cuproptosis regulators. HCC samples from TCGA-LIHC database were divided into FNBP4 low and FNBP4 high groups based on the median FNBP4 expression level, and the mRNA expression levels of 10 cuproptosis regulators were analyzed between the two groups (Figure 3C). Among them, FDX1 was highly expressed in the FNBP4 low group; LIPT1, DLD, DLAT, PDHB, MTF1, GLS, and CDKN2A were highly expressed in the FNBP4 high group; and the expression levels of LIAS and PDHA1 were not significantly different between the two groups. Therefore, eight genes including

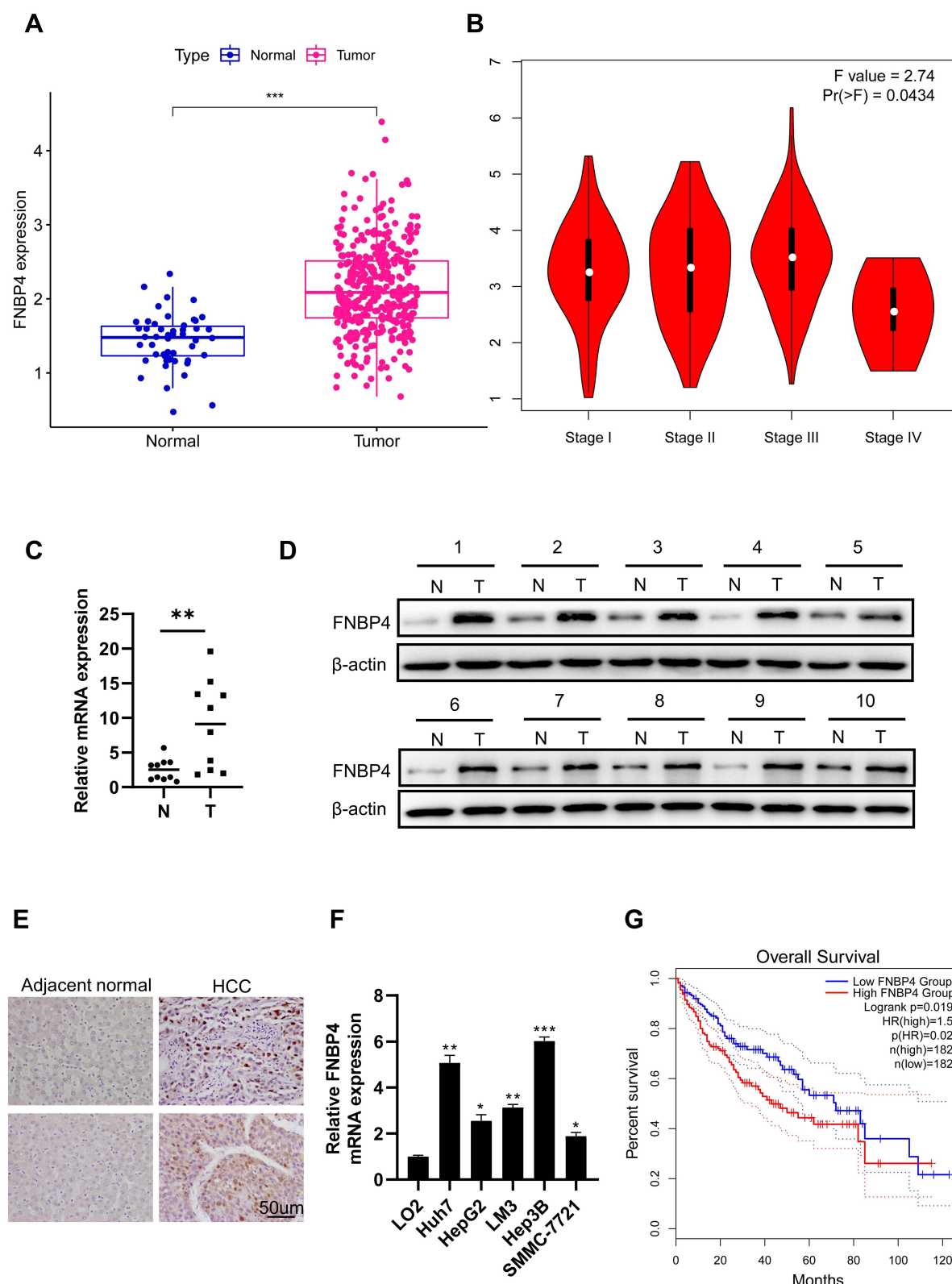


Figure 1 FBNP4 is highly expressed in patients with HCC and is positively correlated with poor OS. **(A)** The expression levels of FBNP4 in HCC (n=374) and adjacent normal tissues (n=50) in the TCGA database. **(B)** The expression levels of FBNP4 in patients with HCC at different pathological stages. **(C)** Quantitative real-time PCR (qRT-PCR) was used to measure the mRNA expression of FBNP4 in 10 pairs of HCC tumor tissues (T) and adjacent normal tissues (N). **(D)** Western blot was used to measure the protein expression of FBNP4 in 10 pairs of HCC tumor tissues (T) and adjacent normal tissues (N). **(E)** Immunohistochemical staining revealed that FBNP4 was upregulated in HCC tissues (n=10). **(F)** qRT-PCR was used to measure the mRNA expression of FBNP4 in five HCC cell lines (Huh7, HepG2, LM3, Hep3B, and SMMC-7721) compared with the normal hepatocyte cell line LO2. **(G)** Kaplan-Meier curve was used to assess the correlation between FBNP4 and overall survival (OS) of the HCC patients in the TCGA database. Data were expressed as Mean \pm SEM. * $p < 0.05$, ** $p < 0.01$, *** $p < 0.001$.

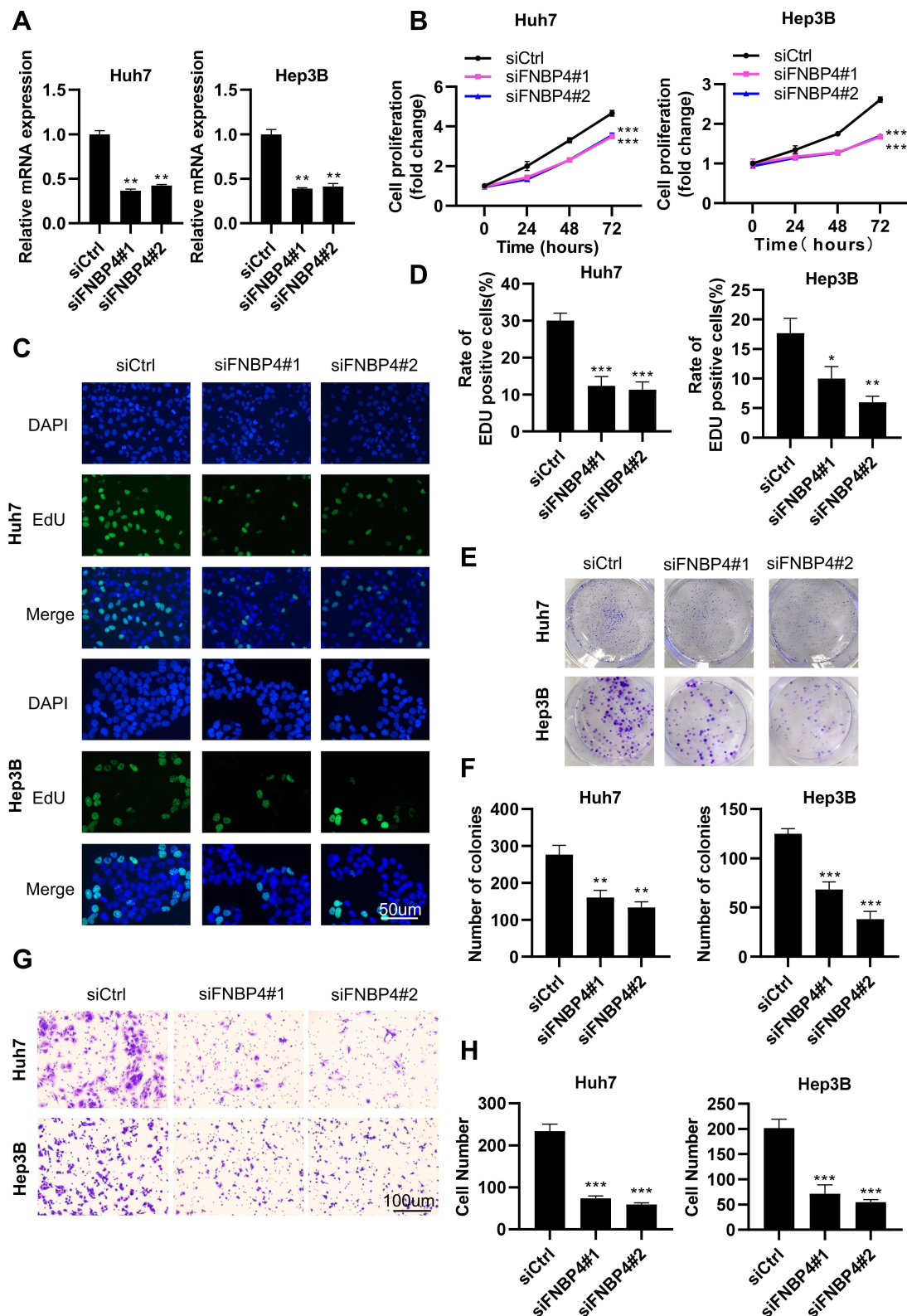


Figure 2 Knockdown of FNBP4 inhibits the proliferation and migration of HCC cells. (A) Huh7 and Hep3B cells were transfected with siControl (siCtrl) or siRNA targeting FNBP4 (siFNBP4) for 48 hrs. qRT-PCR was used to measure the silencing efficiency of siFNBP4 in Huh7 and Hep3B cells. (B) After transfection, Huh7 and Hep3B cells were continued in the medium at specified time points, and cell proliferation was assessed by MTT assays. (C and D) Huh7 and Hep3B cells were transfected with siCtrl or siFNBP4 for 24 hrs and cell proliferation was assessed by 5-Ethynyl-2'-deoxyuridine (EdU) incorporation assay. The percentage of EdU positive cells was quantified. (E and F) Huh7 and Hep3B cells were treated as in (A). A portion of cells were plated into six-well plates (1000 cells/well) and colonies counted after 14 days. The number of colonies was quantified. (G and H) Cell migration was analyzed in Huh7 and Hep3B cells transfected with siCtrl or siFNBP4 by Transwell assay. The number of cells in the chamber was quantified. Data were expressed as Mean \pm SEM. * $p < 0.05$, ** $p < 0.01$, *** $p < 0.001$.

A

FDR ≤ 0.05 FDR > 0.05

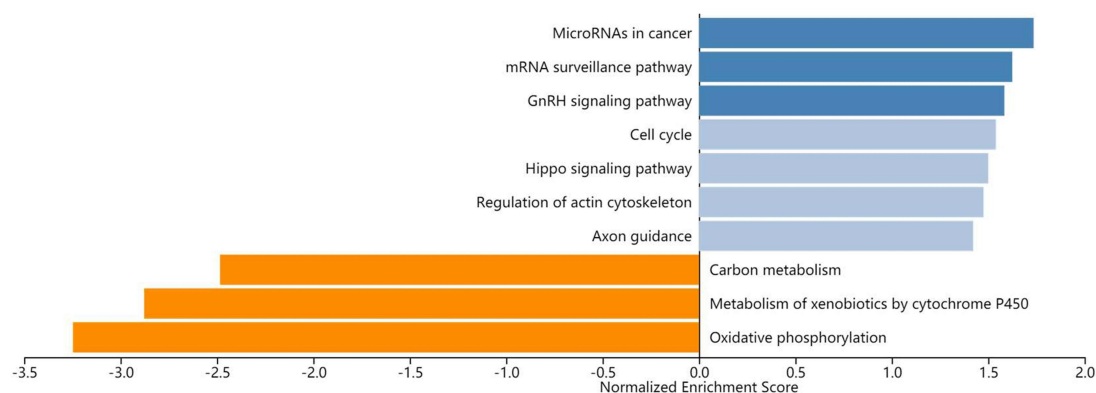
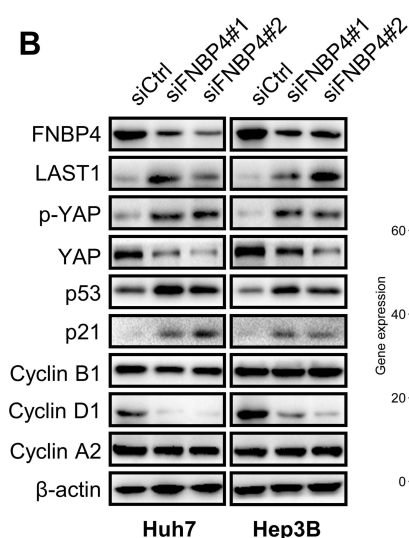
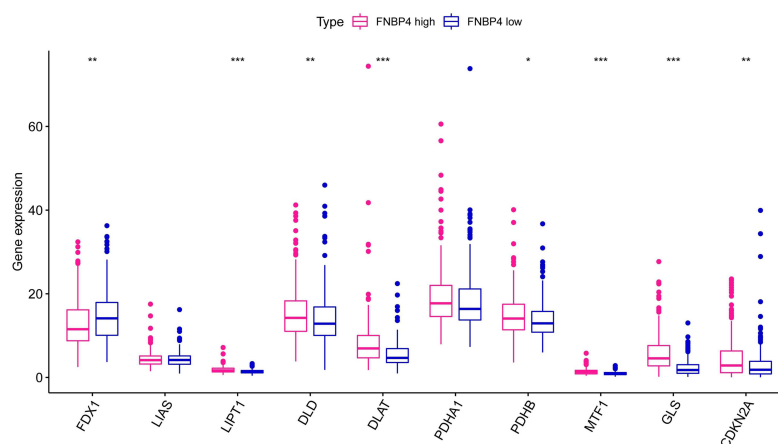
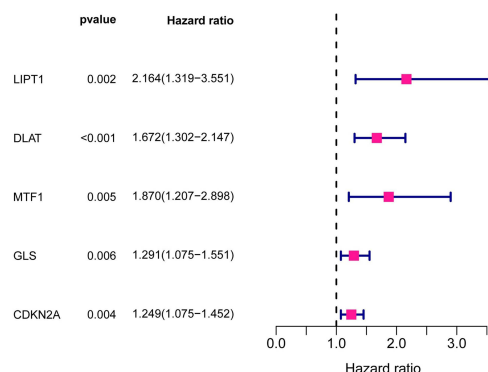
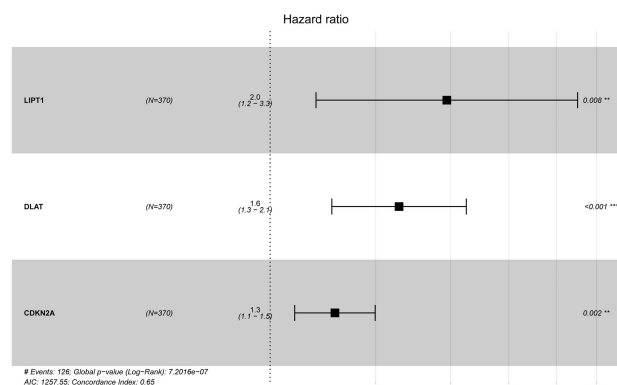
**B****C****D****E**

Figure 3 FBNP4 is associated with tumor-related signaling pathways and cuproptosis regulators in HCC. **(A)** The KEGG pathway analysis was performed with coexpressed genes of FBNP4 in HCC using GESA tools in LinkedOmics. **(B)** The protein expression levels of cell cycle-associated markers (p53, p21, Cyclin B1, Cyclin D1, and Cyclin A2) and the hippo signaling pathway components (LAST1, p-YAP and YAP) were measured by Western blot in Huh7 and Hep3B cells transfected with siCtrl or siFBNP4. **(C)** The expression levels of 10 cuproptosis regulators were analyzed between FBNP4 low and FBNP4 high groups in HCC samples from TCGA-LIHC database. **(D and E)** The univariate **(C)** and multivariate **(D)** Cox regression analyses were performed to determine the prognostic value of the FBNP4-related DECRs in TCGA-LIHC. Data were expressed as Mean ± SEM. * $p < 0.05$, ** $p < 0.01$, *** $p < 0.001$.

FDX1, LIPT1, DLD, DLAT, PDHB, MTF1, GLS, and CDKN2A were defined as FNBP4-related DECRs. To determine the prognostic value of the FNBP4-related DECRs in TCGA-LIHC, we performed a Cox regression analysis, and three genes (LIPT1, DLAT, CDKN2A) were identified as independent risk factors for HCC prognosis (Figure 3D and E).

Construction of a Prognostic Risk Signature Based on FNBP4-Related Cuproptosis Regulators

Next, LIPT1, DLAT, and CDKN2A were used to construct a prognostic risk signature. The risk score for each sample was defined as follows: risk score = sum of the expression levels of the three cuproptosis regulators \times their respective coefficients. Then, patients with HCC were divided into high-risk and low-risk groups according to the median risk score. The Kaplan-Meier survival curve showed that patients in the high-risk group had a significantly worse OS than those in the low-risk group (Figure 4A). The scatter plots show that the expression levels of the three cuproptosis regulators were upregulated in the high-risk group, and the patients in the high-risk group had higher mortality (Figure 4B). Cox regression analysis was performed to determine whether the prognostic risk signature was an independent risk factor for patient prognosis. By incorporating age, gender, grade, and stage into the multivariate Cox regression model, we found that the risk score was an independent prognostic factor for OS of patients with HCC (Figure 4C and D). Furthermore, the ROC curve indicated that the risk score had an area under the curve (AUC) of 0.618, with good clinical prediction efficiency (Figure 4E).

To better apply the risk signature in a clinical setting, we constructed a nomogram including the risk score and clinicopathological characteristics (gender, grade, stage, and TNM) for predicting OS of patients with HCC (Figure 5A). The calibration curves at one, three, and five years showed that the nomogram could accurately predict the prognosis of patients with HCC (Figure 5B).

Discussion

As one of the most common malignant tumors, HCC seriously affects human health. Despite continuous improvements in diagnosis and treatment, the 5-year survival rate of patients with HCC is still not optimal due to delayed diagnosis, high malignancy of cancer cells, and postoperative recurrence.³³ Molecular targeted therapy provides a new treatment hope for patients with unresectable liver cancer. However, HCC progression is a complex multifactorial process involving the accumulation of different types of damage, complex signal transduction, and heterogeneity.^{34–36} Therefore, exploring the key molecules and mechanisms involved in the occurrence and development of HCC is necessary to improve the effectiveness of diagnosis and treatment.

FNBP4, a member of the FBP family, is involved in the regulation of cytoskeletal dynamics during cell division and migration. One study found that FNBP4 was highly expressed in apoptotic mouse T cells, suggesting a possible important role in cell death.¹⁸ However, the intrinsic function and molecular mechanism of action of FNBP4 in tumors are still unknown. It is of great clinical significance to identify novel promising prognostic biomarkers and to explore their roles using bioinformatics methods.^{37,38} In this study, we first found that FNBP4 was highly expressed in patients with HCC from TCGA and our center. In addition, patients with HCC with high expression of FNBP4 had a shorter OS in the TCGA cohort, suggesting that FNBP4 is a potential activator that promotes tumor progression.

Cell proliferation and migration ability are important indicators for the prognostic evaluation of patients with HCC. Therefore, we explored this and observed that downregulation of FNBP4 inhibited HCC proliferation and migration in vitro. Furthermore, our results confirmed that FNBP4 is involved in the regulation of tumor-related signaling pathways, including the cell cycle and the hippo signaling pathway. Cell cycle progression is catalyzed by cyclins and cyclin-dependent kinases.³⁹ Our study found knockdown FNBP4 downregulated the cyclin D1 and upregulated the cell cycle negative regulators p53 and p21, but did not induce a significant change for cyclin B1 and cyclin A2. Cyclin D1, a subtype of cyclin D, forms complexes with cyclin-dependent kinase 4/6 (CDK4/6) and triggers phosphorylation of the retinoblastoma protein (Rb) to release the transcription factor E2F and promote the G1-to-S phase transition.^{40,41} Cyclin D1 accumulation is dysregulated in a variety of human tumors.^{39,42} Therefore, FNBP4 could break the normal cell cycle control, particularly dysregulation of G1/S transition, ultimately leading to uncontrolled cell proliferation and tumorigenesis. The hippo signaling pathway regulates the dynamic balance between cell proliferation and apoptosis and controls the development of tissues and organs as well as the generation of tumors.⁴³ We found

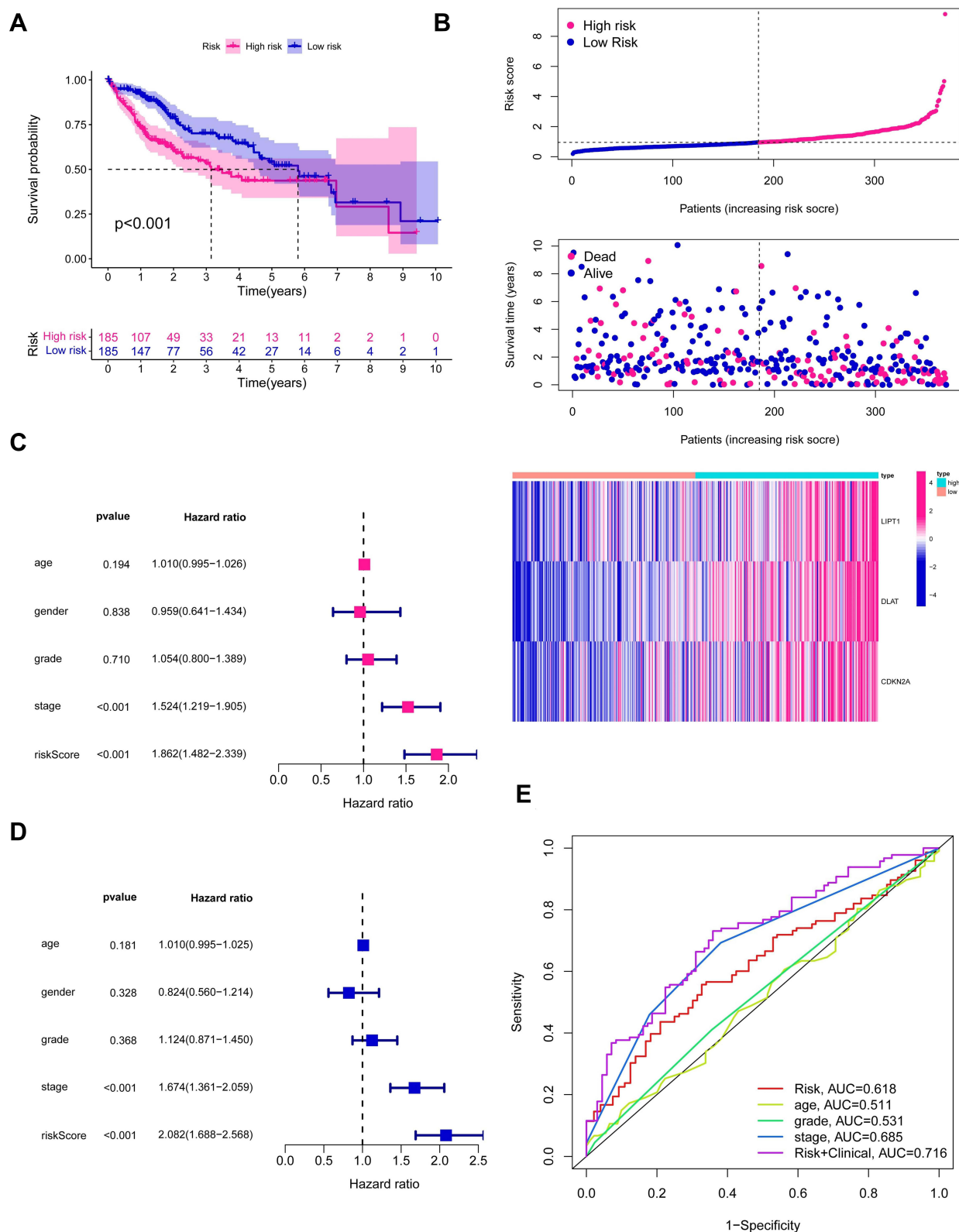


Figure 4 Construction of a prognostic risk signature based on FBNP4-related cuproptosis regulators. **(A)** Kaplan-Meier curve for risk scores in TCGA-LIHC patients. **(B)** Distribution of risk scores, survival status, and gene expression of signature (LIPT1, DLAT, and CDKN2A) for the TCGA-LIHC patients. **(C and D)** The associations between risk score and OS in TCGA-LIHC patients using univariate **(C)** and multivariate **(D)** Cox regression analysis. **(E)** ROC curves of risk score and other clinicopathological characteristics (age, grade, and stage) for one year in the TCGA-LIHC patients.

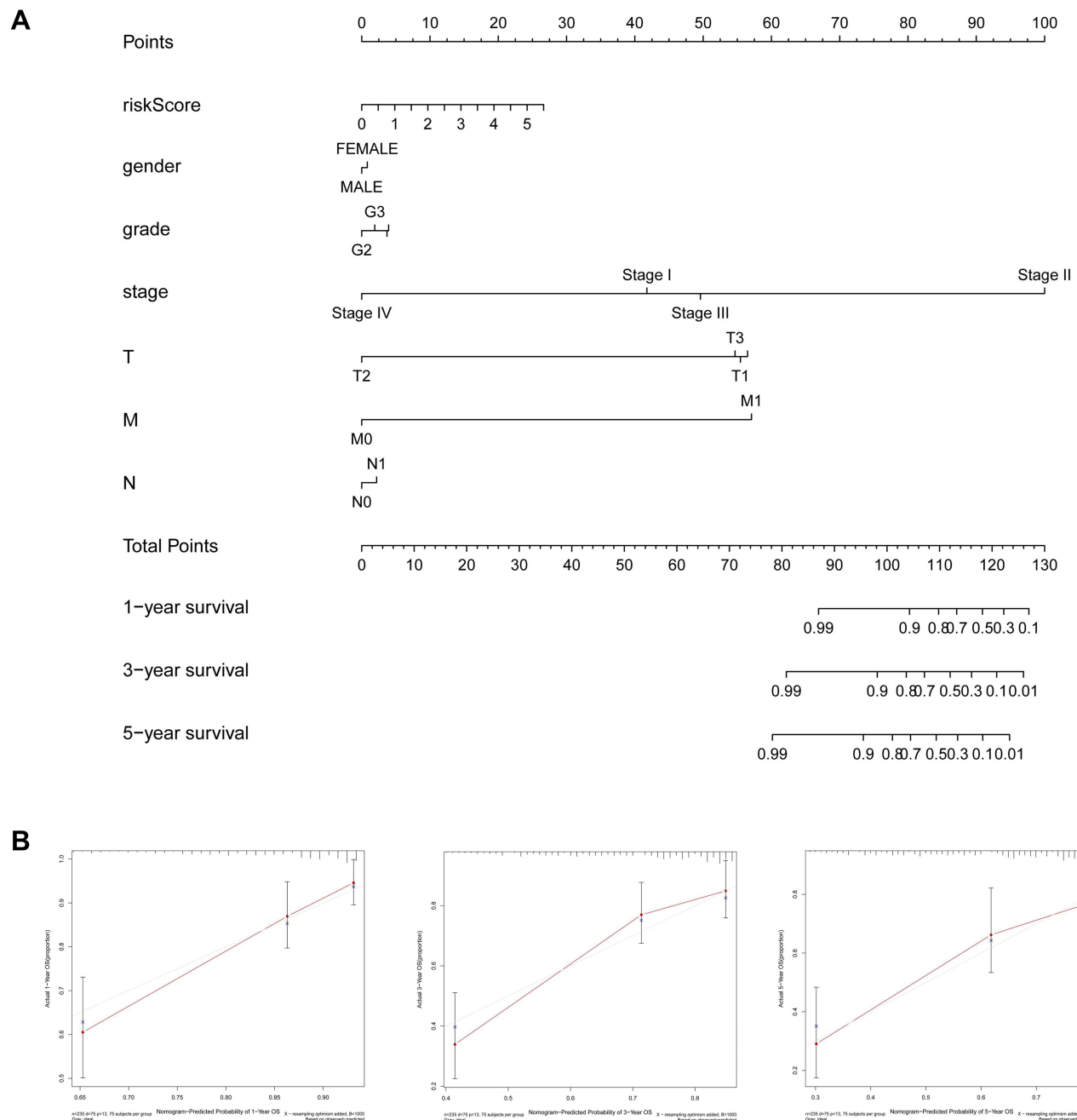


Figure 5 Prognostic nomogram for TCGA-LIHC dataset. **(A)** Nomogram including risk score and clinicopathological characteristics (gender, grade, stage, and TNM) were constructed to predict the survival for TCGA-LIHC patients. **(B)** Calibration curves for nomogram at one, three, and five years. Red line: nomogram-predicted survival curve. Gray line: ideal survival reference curve.

that FBNP4 could inactivate the hippo signaling pathway and cause YAP accumulation. As a core factor of the hippo signaling pathway, YAP plays a crucial role in regulating cell proliferation in cooperation with transcription factors, such as TEAD, SMADs, RUNXs, p63/p73, PAX3, PPARc, TTF1, and TBX-5.^{44–47} Although only in vitro data were obtained in this study, such regulation may exist in the HCC microenvironment. Once this phenomenon is confirmed in vivo, it will imply that FBNP4 plays an essential role in the tumor progression of HCC and make an outstanding contribution to revealing the pathogenesis of HCC.

Cuproptosis has recently been defined as a novel copper-induced cell death mode distinct from apoptosis, necrosis, pyroptosis, and ferroptosis.⁴⁸ As the main organ of copper metabolism, the liver is susceptible to reactions caused by copper accumulation. Excessive copper storage induces the production of free radicals, which can lead to cell damage and even cause

pathological diseases such as Wilson's disease.⁴⁹ Cirrhosis, as a major cause of HCC, is also associated with the accumulation of copper.⁵⁰ However, excessive copper does not inhibit the occurrence and progression of HCC. Therefore, HCC cells may develop a strategy to attenuate the toxicity of increased copper concentrations and avoid the onset of copper-induced cell death. The expression of FDX1 in HCC tumor tissues was lower than that in adjacent normal liver tissue, and knockout of FDX1 resulted in complete loss of protein lipidation and resistance to cuproptosis.^{26,27} However, the regulatory mechanisms of FDX1 and other cuproptosis regulators in HCC are still largely unclear.

In this study, we found that FBNP4 coexpressed genes were significantly enriched in pathways closely related to the TCA cycle, including carbon metabolism, metabolism of xenobiotics by cytochrome P450, and oxidative phosphorylation. Furthermore, copper-induced cell death is closely related to protein lipoylation in the TCA cycle. Therefore, we speculated that FBNP4 is involved in copper-induced cell death and defined a risk signature containing three FBNP4-related DECRs, including LIPT1, DLAT, and CDKN2A, to predict the prognosis of patients with HCC. These three genes play crucial roles in the progression and migration of a variety of tumors. LIPT1, a key gene regulating lipoic acid transport, regulates the TCA cycle in cancer cells.⁵¹ A recent study showed that the expression of LIPT1 not only effectively predicts the prognosis of patients with HCC but also may become a therapeutic target for HCC.⁵² DLAT, a key gene that catalyzes the conversion of pyruvate to acetyl CoA, can enhance ATP production and promote tumor cell proliferation.⁵³ CDKN2A, encoding the cyclin inhibitor p16, binds to cyclin and cyclin-dependent kinases 4 and 6 to inhibit proliferation in normal cells.⁵⁴ However, p16 may play a different role in tumor cells, and CDKN2A can be used as a biomarker for poor prognosis in patients with colon cancer and HCC.⁵⁵ This risk signature is not only an independent risk factor for OS among patients with HCC but also presents good prediction performance. In addition, a nomogram consisting of the risk score and clinicopathological factors was constructed to clinically predict patient prognosis. These findings revealed the potential mechanism of action of FBNP4 in HCC and demonstrated that blockade of FBNP4 is a strong candidate to improve the survival of HCC patients. However, the clear mechanisms by which FBNP4 regulated the HCC cuproptosis needed to be further illustrated using experimental evidence.

Conclusion

We first defined that FBNP4 is a potential prognostic biomarker associated with cuproptosis in HCC. FBNP4 acts as an onco-promoter to promote the proliferation and migration of HCC cells. Future research will focus on the development of molecular targeted drugs for FBNP4 to prevent the progression, invasion, and metastasis of HCC.

Abbreviations

HCC, Hepatocellular carcinoma; FBNP4, formin-binding protein 4; KEGG, Kyoto Encyclopedia of Genes and Genomes; OS, overall survival; DECRs, differentially expressed cuproptosis regulators; NAFLD, non-alcoholic fatty liver disease; FBNPs/FBPs, formin-binding proteins; TCA, tricarboxylic acid; FDX1, ferredoxin 1; TCGA-LIHC, The Cancer Genome Atlas-Liver hepatocellular carcinoma; FPKM, Fragments per kilobase million; GEPIA2, Gene Expression Profiling Interactive Analysis 2; ROC, receiver operating characteristic; BSA, bovine serum albumin; AUC, area under the curve; CDK4/6, cyclin-dependent kinase 4/6, Rb, retinoblastoma protein.

Data Sharing Statement

All the data generated during this study are available from the corresponding authors on reasonable request.

Ethics Approval

All experiments were approved by the ethics committee of the Second Affiliated Hospital of Chongqing Medical University.

Acknowledgments

We thank Key Laboratory of Hepatobiliary and Pancreatic Surgery of Army Medical University for research equipment and technical support for this research.

Author Contributions

All authors made a significant contribution to the work reported, whether that is in the conception, study design, execution, acquisition of data, analysis and interpretation, or in all these areas; took part in drafting, revising or critically reviewing the article; gave final approval of the version to be published; have agreed on the journal to which the article has been submitted; and agree to be accountable for all aspects of the work.

Disclosure

All authors declare no conflicts of interest in this work.

References

1. Zhang Y, Zhang S, Liu J, et al. Identification of serum glycobiomarkers for Hepatocellular Carcinoma using lectin microarrays. *Front Immunol.* 2022;13:973993. doi:10.3389/fimmu.2022.973993
2. Luna-Marco C, Ubink A, Kopsida M, Heindryckx F. Endoplasmic Reticulum Stress and Metabolism in Hepatocellular Carcinoma. *Am J Pathol.* 2022. doi:10.1016/j.ajpath.2022.09.012
3. Cho K, Ro SW, Seo SH, et al. Genetically Engineered Mouse Models for Liver Cancer. *Cancers.* 2019;12(1):14. doi:10.3390/cancers12010014
4. Llovet JM, Castet F, Heikenwalder M, et al. Immunotherapies for hepatocellular carcinoma. *Nat Rev Clin Oncol.* 2022;19(3):151–172. doi:10.1038/s41571-021-00573-2
5. Di Federico A, Rizzo A, Carloni R, et al. Atezolizumab-bevacizumab plus Y-90 TARE for the treatment of hepatocellular carcinoma: preclinical rationale and ongoing clinical trials. *Expert Opin Investig Drugs.* 2022;31(4):361–369. doi:10.1080/13543784.2022.2009455
6. Viscardi G, Tralongo AC, Massari F, et al. Comparative assessment of early mortality risk upon immune checkpoint inhibitors alone or in combination with other agents across solid malignancies: a systematic review and meta-analysis. *Eur J Cancer.* 2022;177:175–185. doi:10.1016/j.ejca.2022.09.031
7. Li D, Toh HC, Merle P, et al. Atezolizumab plus Bevacizumab versus Sorafenib for Unresectable Hepatocellular Carcinoma: results from Older Adults Enrolled in the IMbrave150 Randomized Clinical Trial. *Liver Cancer.* 2022;11(6):558–571. doi:10.1159/000525671
8. Rizzo A, Ricci AD, Di Federico A, et al. Predictive Biomarkers for Checkpoint Inhibitor-Based Immunotherapy in Hepatocellular Carcinoma: where Do We Stand? *Front Oncol.* 2021;11:803133. doi:10.3389/fonc.2021.803133
9. Li J, Xie J, Wu D, et al. A pan-cancer analysis revealed the role of the SLC16 family in cancer. *Channels.* 2021;15(1):528–540. doi:10.1080/19336950.2021.1965422
10. Cammarota A, Zanuso V, Manfredi GF, Murphy R, Pinato DJ, Rimassa L. Immunotherapy in hepatocellular carcinoma: how will it reshape treatment sequencing? *Ther Adv Med Oncol.* 2023;15:17588359221148029. doi:10.1177/17588359221148029
11. Rizzo A, Nannini M, Novelli M, Dalia Ricci A, Scioscio VD, Pantaleo MA. Dose reduction and discontinuation of standard-dose regorafenib associated with adverse drug events in cancer patients: a systematic review and meta-analysis. *Ther Adv Med Oncol.* 2020;12:1758835920936932. doi:10.1177/1758835920936932
12. Faix J, Grosse R. Staying in shape with formins. *Dev Cell.* 2006;10(6):693–706. doi:10.1016/j.devcel.2006.05.001
13. Ahangar P, Cowin AJ. Reforming the Barrier: the Role of Formins in Wound Repair. *Cells.* 2022;11(18):2779. doi:10.3390/cells11182779
14. Chiareghin C, Robusto M, Massa V, et al. Role of Cytoskeletal Diaphanous-Related Formins in Hearing Loss. *Cells.* 2022;11(11):1726. doi:10.3390/cells11111726
15. Young KG, Copeland JW. Formins in cell signaling. *Biochim Biophys Acta.* 2010;1803(2):183–190. doi:10.1016/j.bbamer.2008.09.017
16. Yoon BK, Hwang N, Chun KH, et al. Sp1-Induced FBNP1 Drives Rigorous 3D Cell Motility in EMT-Type Gastric Cancer Cells. *Int J Mol Sci.* 2021;22(13):6784. doi:10.3390/ijms22136784
17. Suman P, Mishra S, Chander H. High expression of FBP17 in invasive breast cancer cells promotes invadopodia formation. *Med Oncol.* 2018;35(5):71. doi:10.1007/s12032-018-1132-5
18. Depraetere V, Golstein P. WW domain-containing FBP-30 is regulated by p53. *Cell Death Differ.* 1999;6(9):883–889. doi:10.1038/sj.cdd.4400564
19. Song S, Zhang M, Xie P, Wang S, Wang Y. Comprehensive analysis of cuproptosis-related genes and tumor microenvironment infiltration characterization in breast cancer. *Front Immunol.* 2022;13:978909. doi:10.3389/fimmu.2022.978909
20. Feng W, Su S, Song C, et al. Effects of Copper Exposure on Oxidative Stress, Apoptosis, Endoplasmic Reticulum Stress, Autophagy and Immune Response in Different Tissues of Chinese Mitten Crab (*Eriocheir sinensis*). *Antioxidants.* 2022;11(10). doi:10.3390/antiox11102029
21. Siddiqui MA, Alhadlaq HA, Ahmad J, Al-Khedhairi AA, Musarrat J, Ahamed M. Copper oxide nanoparticles induced mitochondria mediated apoptosis in human hepatocarcinoma cells. *PLoS One.* 2013;8(8):e69534. doi:10.1371/journal.pone.0069534
22. Kuo HW, Chen SF, Wu CC, Chen DR, Lee JH. Serum and tissue trace elements in patients with breast cancer in Taiwan. *Biol Trace Elem Res.* 2002;89(1):1–11. doi:10.1385/bter:89:1:1
23. Zhang X, Yang Q. Association between serum copper levels and lung cancer risk: a meta-analysis. *J Int Med Res.* 2018;46(12):4863–4873. doi:10.1177/0300060518798507
24. Moffett JR, Puthillathu N, Vengilote R, Jaworski DM, Namboodiri AM. Acetate Revisited: a Key Biomolecule at the Nexus of Metabolism, Epigenetics and Oncogenesis-Part 1: acetyl-CoA, Acetogenesis and Acyl-CoA Short-Chain Synthetases. *Front Physiol.* 2020;11:580167. doi:10.3389/fphys.2020.580167
25. Koizumi M, Fujii J, Suzuki K, et al. A marked increase in free copper levels in the plasma and liver of LEC rats: an animal model for Wilson disease and liver cancer. *Free Radic Res.* 1998;28(5):441–450. doi:10.3109/10715769809066881
26. Tsvetkov P, Coy S, Petrova B, et al. Copper induces cell death by targeting lipoylated TCA cycle proteins. *Science.* 2022;375(6586):1254–1261. doi:10.1126/science.abf0529
27. Zhang Z, Zeng X, Wu Y, Liu Y, Zhang X, Song Z. Cuproptosis-Related Risk Score Predicts Prognosis and Characterizes the Tumor Microenvironment in Hepatocellular Carcinoma. *Front Immunol.* 2022;13:925618. doi:10.3389/fimmu.2022.925618

28. Peng X, Zhu J, Liu S, et al. Signature construction and molecular subtype identification based on cuproptosis-related genes to predict the prognosis and immune activity of patients with hepatocellular carcinoma. *Front Immunol.* **2022**;13:990790. doi:10.3389/fimmu.2022.990790
29. Wang G, Xiao R, Zhao S, et al. Cuproptosis regulator-mediated patterns associated with immune infiltration features and construction of cuproptosis-related signatures to guide immunotherapy. *Front Immunol.* **2022**;13:945516. doi:10.3389/fimmu.2022.945516
30. Chen D, Cui QC, Yang H, Dou QP. Disulfiram, a clinically used anti-alcoholism drug and copper-binding agent, induces apoptotic cell death in breast cancer cultures and xenografts via inhibition of the proteasome activity. *Cancer Res.* **2006**;66(21):10425–10433. doi:10.1158/0008-5472.Can-06-2126
31. O'Day SJ, Eggermont AM, Chiarion-Sileni V, et al. Final results of Phase III SYMMETRY study: randomized, double-blind trial of elesclomol plus paclitaxel versus paclitaxel alone as treatment for chemotherapy-naïve patients with advanced melanoma. *J Clin Oncol.* **2013**;31(9):1211–1218. doi:10.1200/jco.2012.44.5585
32. Chen L, Min J, Wang F. Copper homeostasis and cuproptosis in health and disease. *Signal Transduct Target Ther.* **2022**;7(1):378. doi:10.1038/s41392-022-01229-y
33. Yang JC, Hu JJ, Li YX, Luo W, Liu JZ, Ye DW. Clinical Applications of Liquid Biopsy in Hepatocellular Carcinoma. *Front Oncol.* **2022**;12:781820. doi:10.3389/fonc.2022.781820
34. Feng H, Zhuo Y, Zhang X, et al. Tumor Microenvironment in Hepatocellular Carcinoma: key Players for Immunotherapy. *J Hepatocell Carcinoma.* **2022**;9:1109–1125. doi:10.2147/jhc.S381764
35. Dash S, Aydin Y, Wu T. Integrated stress response in hepatitis C promotes Nrf2-related chaperone-mediated autophagy: a novel mechanism for host-microbe survival and HCC development in liver cirrhosis. *Semin Cell Dev Biol.* **2020**;101:20–35. doi:10.1016/j.semedb.2019.07.015
36. Shokouhian B, Aboulkheyr EH, Negahdari B, et al. Hepatogenesis and hepatocarcinogenesis: alignment of the main signaling pathways. *J Cell Physiol.* **2022**;237(11):3984–4000. doi:10.1002/jcp.30862
37. Xie J, Zhu Z, Cao Y, Ruan S, Wang M, Shi J. Solute carrier transporter superfamily member SLC16A1 is a potential prognostic biomarker and associated with immune infiltration in skin cutaneous melanoma. *Channels.* **2021**;15(1):483–495. doi:10.1080/19336950.2021.1953322
38. Xie J, Ruan S, Zhu Z, et al. Database mining analysis revealed the role of the putative H(+)/sugar transporter solute carrier family 45 in skin cutaneous melanoma. *Channels.* **2021**;15(1):496–506. doi:10.1080/19336950.2021.1956226
39. Qie S, Yoshida A, Parnham S, et al. Targeting glutamine-addiction and overcoming CDK4/6 inhibitor resistance in human esophageal squamous cell carcinoma. *Nat Commun.* **2019**;10(1):1296. doi:10.1038/s41467-019-09179-w
40. Tchakarska G, Sola B. The double dealing of cyclin D1. *Cell Cycle.* **2020**;19(2):163–178. doi:10.1080/15384101.2019.1706903
41. Montalto FI, De Amicis F. Cyclin D1 in Cancer: a Molecular Connection for Cell Cycle Control, Adhesion and Invasion in Tumor and Stroma. *Cells.* **2020**;9:12. doi:10.3390/cells9122648
42. Qie S, Diehl JA. Cyclin D1, cancer progression, and opportunities in cancer treatment. *J Mol Med.* **2016**;94(12):1313–1326. doi:10.1007/s00109-016-1475-3
43. Yu FX, Zhao B, Guan KL. Hippo Pathway in Organ Size Control, Tissue Homeostasis, and Cancer. *Cell.* **2015**;163(4):811–828. doi:10.1016/j.cell.2015.10.044
44. Chen D, Sun Y, Wei Y, et al. LIFR is a breast cancer metastasis suppressor upstream of the Hippo-YAP pathway and a prognostic marker. *Nat Med.* **2012**;18(10):1511–1517. doi:10.1038/nm.2940
45. Hao Y, Chun A, Cheung K, Rashidi B, Yang X. Tumor suppressor LATS1 is a negative regulator of oncogene YAP. *J Biol Chem.* **2008**;283(9):5496–5509. doi:10.1074/jbc.M709037200
46. Lamar JM, Stern P, Liu H, Schindler JW, Jiang ZG, Hynes RO. The Hippo pathway target, YAP, promotes metastasis through its TEAD-interaction domain. *Proc Natl Acad Sci U S A.* **2012**;109(37):E2441–2450. doi:10.1073/pnas.1212021109
47. Kim NG, Koh E, Chen X, Gumbiner BM. E-cadherin mediates contact inhibition of proliferation through Hippo signaling-pathway components. *Proc Natl Acad Sci U S A.* **2011**;108(29):11930–11935. doi:10.1073/pnas.1103345108
48. Duan WJ, He RR. Cuproptosis: copper-induced regulated cell death. *Sci China Life Sci.* **2022**;65(8):1680–1682. doi:10.1007/s11427-022-2106-6
49. Kodama H, Fujisawa C, Bhadrprasit W. Inherited copper transport disorders: biochemical mechanisms, diagnosis, and treatment. *Curr Drug Metab.* **2012**;13(3):237–250. doi:10.2174/138920012799320455
50. Poznański J, Słodacki D, Czarkowska-Pączek B, et al. Cirrhotic Liver of Liver Transplant Recipients Accumulate Silver and Co-Accumulate Copper. *Int J Mol Sci.* **2021**;22(4):1782. doi:10.3390/ijms22041782
51. Mayr JA, Feichtinger RG, Tort F, Ribes A, Sperl W. Lipoic acid biosynthesis defects. *J Inherit Metab Dis.* **2014**;37(4):553–563. doi:10.1007/s10545-014-9705-8
52. Yan C, Niu Y, Ma L, Tian L, Ma J. System analysis based on the cuproptosis-related genes identifies LIPT1 as a novel therapy target for liver hepatocellular carcinoma. *J Transl Med.* **2022**;20(1):452. doi:10.1186/s12967-022-03630-1
53. Bai WD, Liu JY, Li M, et al. A Novel Cuproptosis-Related Signature Identified DLAT as a Prognostic Biomarker for Hepatocellular Carcinoma Patients. *World J Oncol.* **2022**;13(5):299–310. doi:10.14740/wjon1529
54. Chen Z, Guo Y, Zhao D, et al. Comprehensive Analysis Revealed that CDKN2A is a Biomarker for Immune Infiltrates in Multiple Cancers. *Front Cell Dev Biol.* **2021**;9:808208. doi:10.3389/fcell.2021.808208
55. Zhou Y, Wang XB, Qiu XP, Shuai Z, Wang C, Zheng F. CDKN2A promoter methylation and hepatocellular carcinoma risk: a meta-analysis. *Clin Res Hepatol Gastroenterol.* **2018**;42(6):529–541. doi:10.1016/j.clinre.2017.07.003

International Journal of General Medicine

Dovepress

Publish your work in this journal

The International Journal of General Medicine is an international, peer-reviewed open-access journal that focuses on general and internal medicine, pathogenesis, epidemiology, diagnosis, monitoring and treatment protocols. The journal is characterized by the rapid reporting of reviews, original research and clinical studies across all disease areas. The manuscript management system is completely online and includes a very quick and fair peer-review system, which is all easy to use. Visit <http://www.dovepress.com/testimonials.php> to read real quotes from published authors.

Submit your manuscript here: <https://www.dovepress.com/international-journal-of-general-medicine-journal>